Supplemental Figures

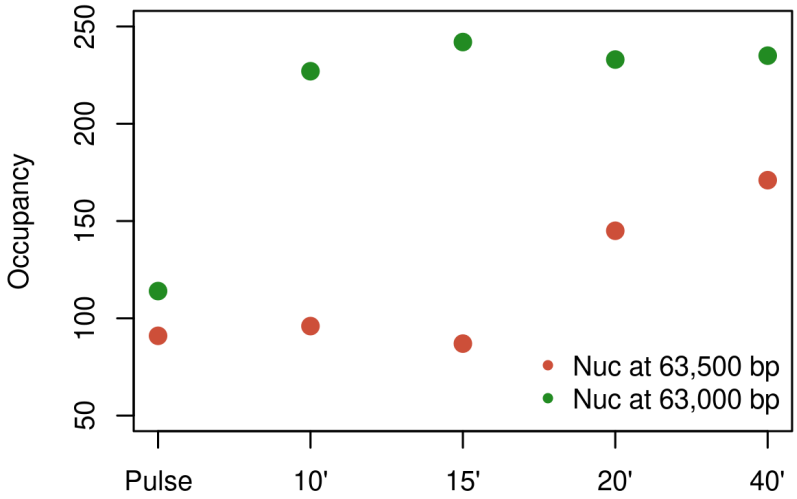

Supplemental Figure 1. NCOP captures nucleosomes assembled at heterogeneous rates in *cac1Δ* cells. Occupancy of nucleosomes positioned at 63,000 bp and 63,500 bp on ChrI in *cac1Δ* cells across all time points.

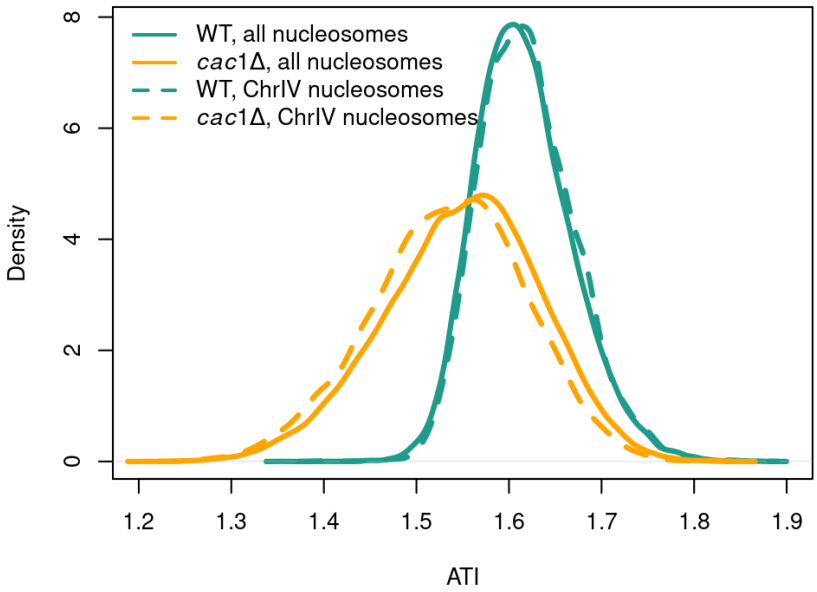

Supplemental Figure 2. Nucleosomes on ChrIV are representative of nucleosomes across the genome. Density distribution of ATI values for all high-confidence nucleosomes and nucleosomes on ChrIV in WT and *cac1Δ* cells.

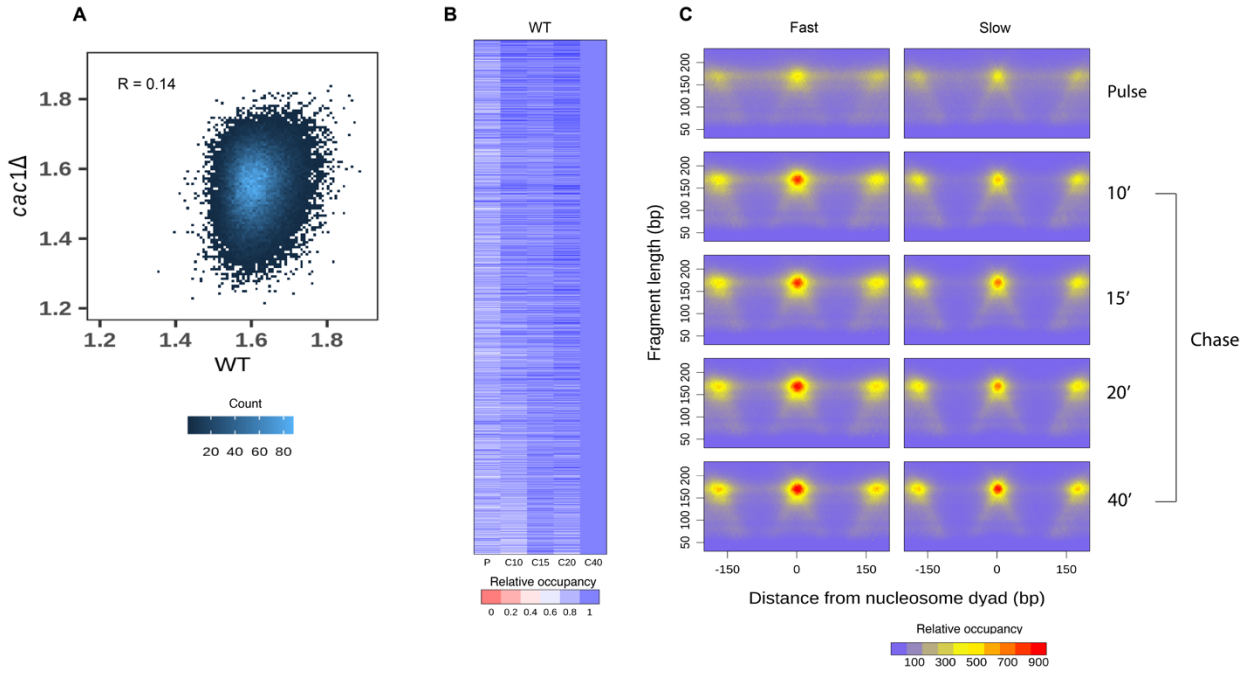

Supplemental Figure 3. Nucleosomal ATI values determined from WT and *cac1Δ* cells are not correlated with each other. (A) Density scatter plot depicting the ATI values for individual nucleosomes from WT and *cac1Δ* cells. (B) Heatmap showing the nucleosome occupancy at each time point relative to the final time point in WT, presented in order of decreasing ATI values determined from *cac1Δ* cells. (C) Aggregate chromatin profiles of slow and fast nucleosomes identified from *cac1Δ* cells using WT data.

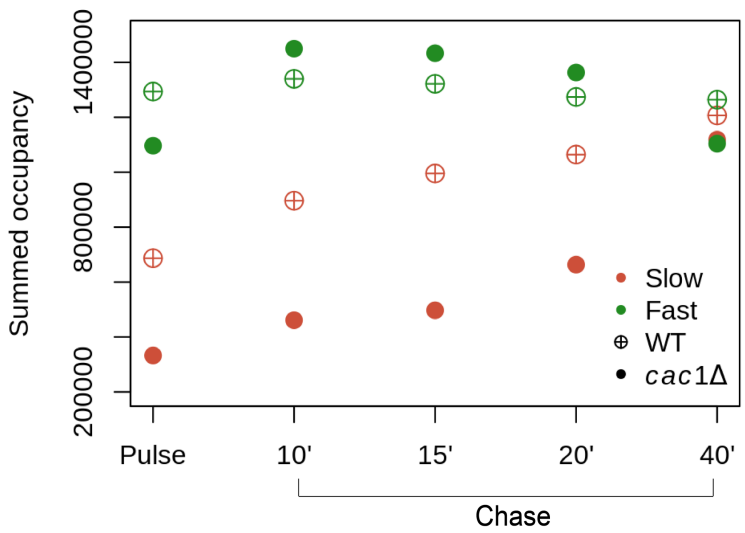

Supplemental Figure 4. Fast and slow nucleosomes identified in *cac1Δ* cells have different maturation kinetics. Summed occupancy of fast and slow nucleosomes identified in WT and *cac1Δ* cells across all time points.

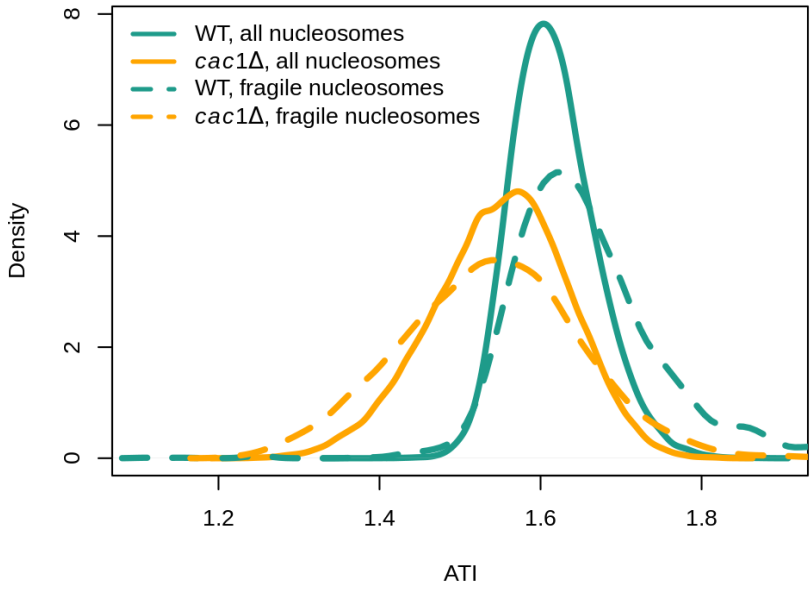

Supplemental Figure 5. Maturation kinetics of nucleosomes are not related to their sensitivity to MNase digestion. Density distribution of ATI values for all high-confidence nucleosomes and fragile nucleosomes in WT and *cac1Δ* cells.

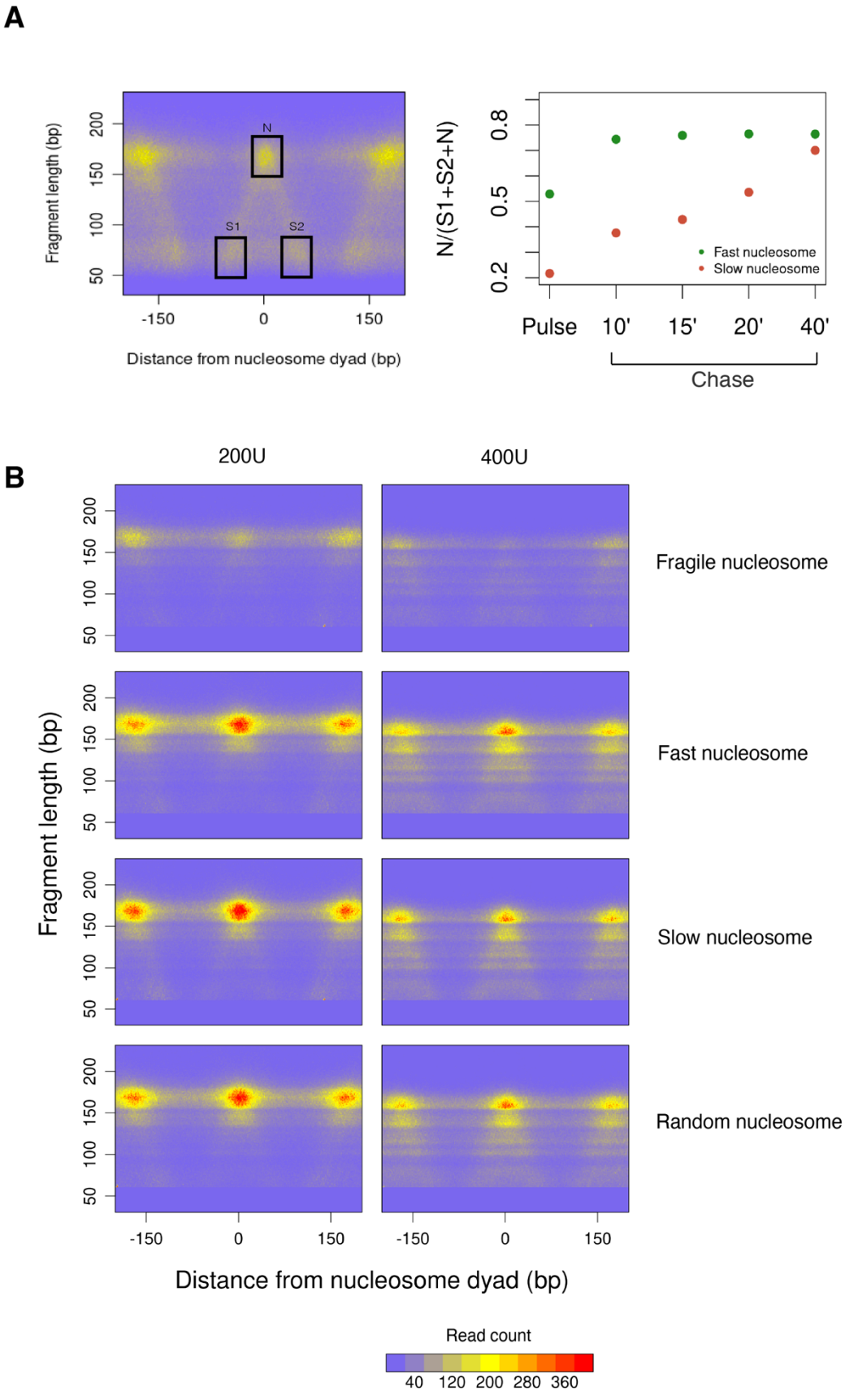
A
Fragment length (bp)
200
150
100
50
N
S1
S2
-150
0
150
Distance from nucleosome dyad (bp)
N/(S1+S2+N)
0.8
0.5
0.2
Fast nucleosome
Slow nucleosome
Pulse
10'
15'
20'
40'
Chase
B
200U
400U
Fragile nucleosome
Fast nucleosome
Slow nucleosome
Random nucleosome
Fragment length (bp)
Distance from nucleosome dyad (bp)
Read count
40 120 200 280 360

Supplemental Figure 6. Slow/fast nucleosomes exhibit distinct signatures from fragile nucleosomes. (A) Discrete nucleosomes (N) and nucleosome subassemblies (S1 and S2) are observed in the MNase data (left panel). The ratio of nucleosomes to nucleosome subassemblies for fast and slow nucleosomes is dynamic across the time course, reflecting the conversion of subassemblies to complete nucleosomes (right panel). (B) Aggregated chromatin profiles of fast, slow, random, and fragile nucleosomes generated from MNase-seq experiments treated with low (200U) and high (400U) concentrations of MNase (Chereji et al. 2017).

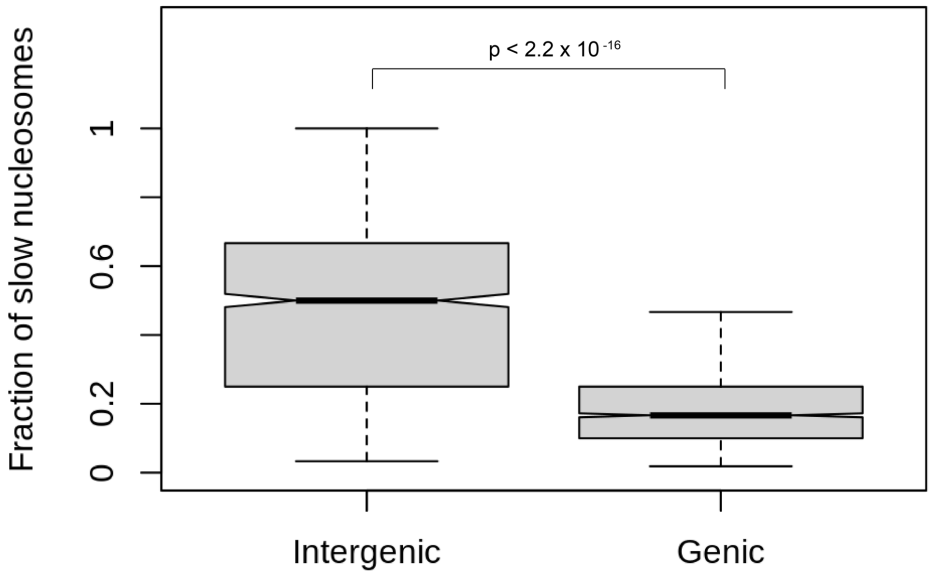

Supplemental Figure 7. Slow nucleosomes are enriched in intergenic regions compared to gene bodies. Boxplot depicting the fraction of slow nucleosomes, identified in *cac1Δ* cells, among all nucleosomes in the intergenic regions and genic regions. The difference between the fraction of slow nucleosomes in the intergenic regions and genic regions is significant ($p < 2.2 \times 10^{-16}$).

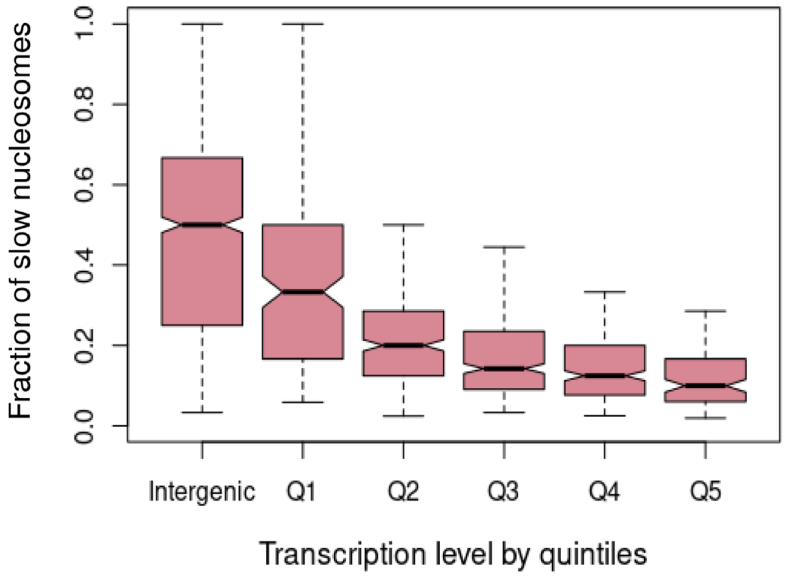

Supplemental Figure 8. Actively transcribed genes are associated with fewer slow nucleosomes regardless of proximity to TSSs. Boxplot depicting the fraction of slow nucleosomes identified in *cac1Δ* cells among all nucleosomes in the intergenic regions and gene bodies, excluding the first 300bp from TSSs.

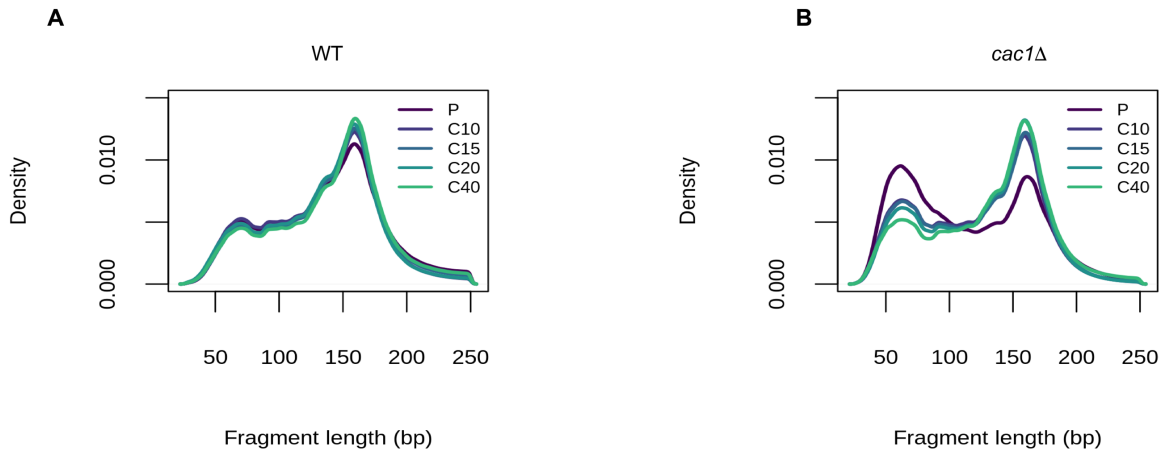

Supplemental Figure 9. The nascent chromatin of *cac1Δ* cells displays an increase in subnucleosomal-sized fragments that gradually disappears as the chromatin matures. Density distribution of fragment length in (A) WT and (B) *cac1Δ* cells at all time points.

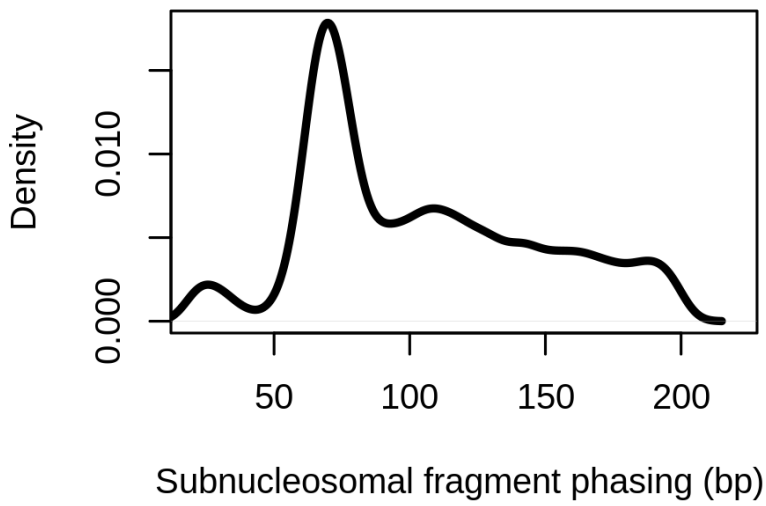

Supplemental Figure 10. Subnucleosomal-sized fragments captured from nascent chromatin in *cac1Δ* cells form ordered arrays of phased clusters. Density distribution of the phasing of subnucleosomal fragments in gene bodies in the nascent chromatin of *cac1Δ* cells.

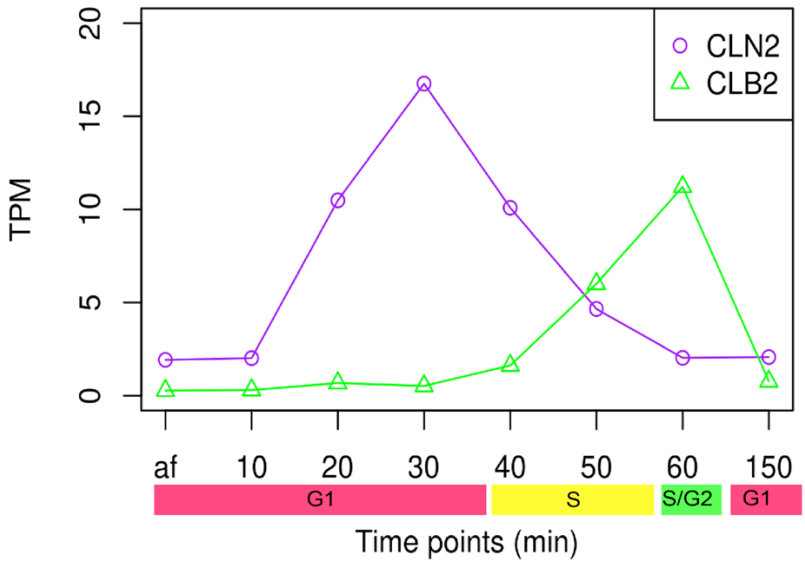

Supplemental Figure 11. Time-course RNA-seq accurately captures the expression patterns of cell cycle genes. Expression levels of Cln2 (purple) and Clb2 (green) over the time course.

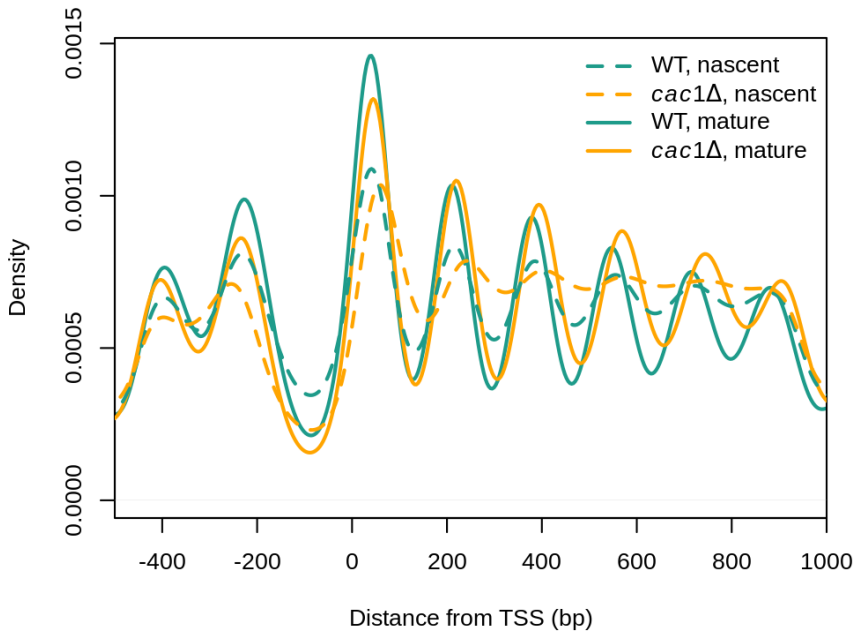

Supplemental Figure 12. Nucleosome occupancy profiles of WT and *cac1Δ* cells after a 5 minute EdU pulse (nascent) and 40 minutes following a thymidine chase (mature).

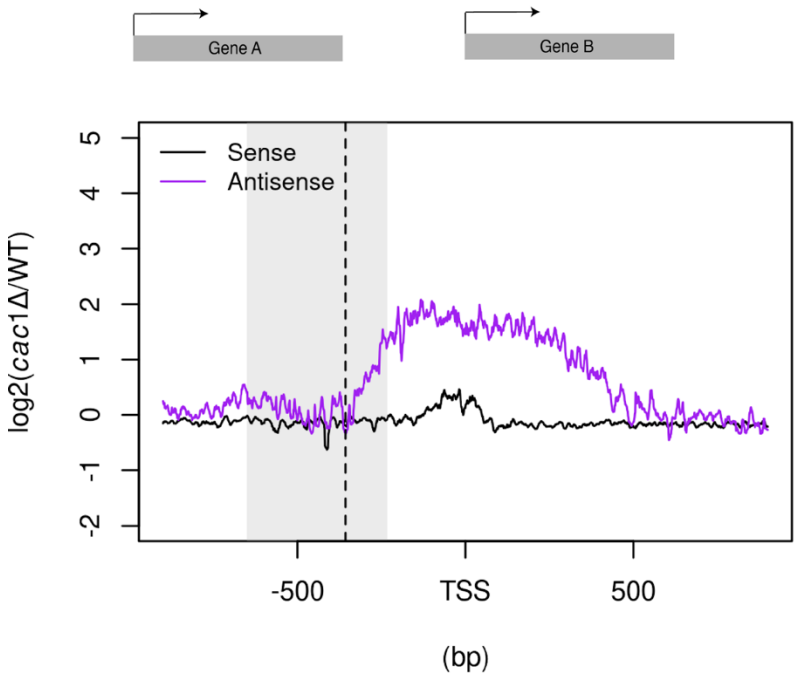

Supplemental Figure 13. Aggregate log2 fold-difference of gene expression between *cac1Δ* cells and WT cells around all tandem gene pairs. Expression signals were aligned to the TSSs of Gene B, as depicted at the top of the figure. The gray shading depicts where the end of Gene A is likely to be found based on the summary statistics of the distance between the ends of Gene A and the TSSs of Gene B— 1st quartile to 3rd quartile with the dashed line denoting the median.

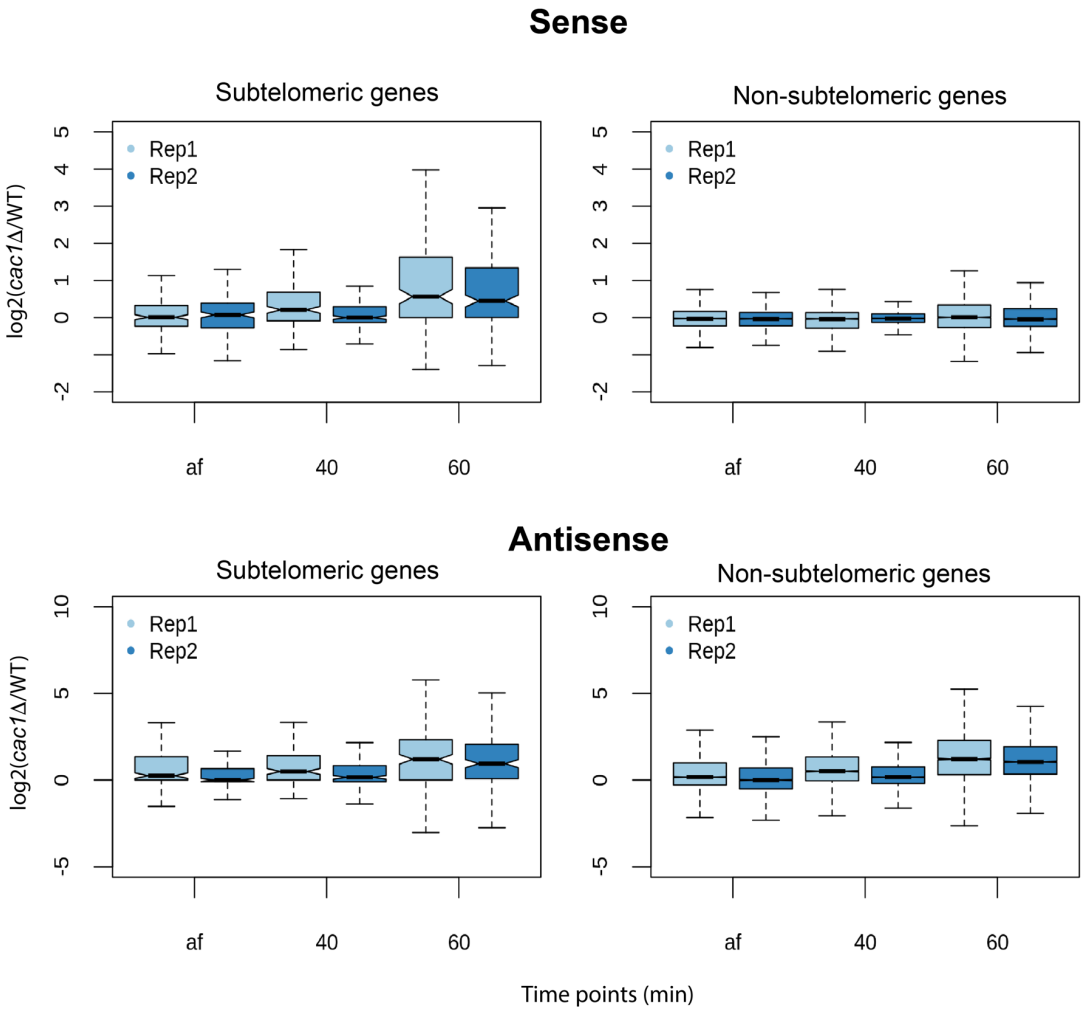

Supplemental Figure 14. Two biological replicates of the RNA-seq experiments are consistent with each other. These four panels show data from experiments undertaken to replicate the results of Figures 5B-E.

References:

Chereji RV, Ocampo J, Clark DJ. 2017. MNase-sensitive complexes in yeast: nucleosomes and non-histone barriers. *Mol Cell* **65**: 565–577.e3.